Journal of Operation and Automation in Power Engineering
Vol. 4, No. 2, Dec. 2016, Pages: 93-103
http://joape.uma.ac.ir

A SAIWD-based Approach for Simultaneous Reconfiguration and Optimal Siting and Sizing of Wind Turbines and DVR units in Distribution Systems

*A. Lashkar Ara [1], H. Bagheri Tolabi [2,]**, *R. Hosseini [3]*

[1] *Department of Electrical Engineering, Dezful Branch, Islamic Azad University, Dezful, Iran*
[2] *Department of Electrical Engineering, Khorramabad Branch, Islamic Azad University, Khorramabad, Iran*
[3] *Department of Computer Engineering, Shahr-e-Qods Branch, Islamic Azad University, Tehran, Iran*

Abstract- *In this paper, a combination of simulated annealing (SA) and intelligent water drops (IWD) algorithm is used to solve the nonlinear/complex problem of simultaneous reconfiguration with optimal allocation (size and location) of wind turbine (WT) as a distributed generation (DG) and dynamic voltage restorer (DVR) as a distributed flexible AC transmission systems* **(***DFACT) unit in a distribution system. The objectives of this research are to minimize active power loss, minimize operational cost, improve voltage stability, and increase the load balancing of the system. For evaluation purposes, the proposed algorithm is evaluated using the Tai-Power 11.4-kV real distribution network. The impacts of the optimal placement of the WT, DVR, and WT with DVR units are separately evaluated. The results are compared in terms of statistical indicators. By comparing all the testing scenarios, it is observed that the multi-objective optimization evolutionary algorithm is more beneficial than its single-objective optimization counterpart. Also, the obtained results show that the proposed SAIWD method outperforms the IWD method and other intelligent search algorithms such as genetic algorithm or particle swarm optimization.*

Keyword: Distribution system**,** Dynamic voltage restorer**,** Intelligent water drops**,** Reconfiguration**,** Simulated annealing**,** Wind turbine.

1. INTRODUCTION

A distribution system consists of two types of switches, i.e. tie (open) and sectionalizing (closed). By changing the status of switches between feeders, the structure of the distribution network will change, which is known as reconfiguration [1]. The main objective of reconfiguration is to reduce losses, increase voltage stability and reliability, improve voltage profile, enhance load balancing, and relieve overload in the distribution network [2].

Merlin and Back first proposed the concept of reconfiguration in a distribution network in 1975 [3]. A genetic algorithm was used for reconfiguration to specify the minimal loss operational structure [4]. This algorithm is more useful for finding the global optimum solution than the heuristic techniques and takes less time than the complete exhaustive search, but its main problem is how to code the objects into strings [4]. Venkatesh and Ranjan [5] proposed a reconfiguration method that uses a fuzzy programming technique. This method is effective for multi-objective problems. Recently, the use of distributed generation resources (i.e. photovoltaic, fuel cells, small wind turbines, etc.) has become very popular and important, especially in restructured power systems. The advantages of distributed generation of resources include reduction in power loss and improvement in voltage profile and reliability of the network. In order to take the most advantage of DG units, the selection of their optimal locations and capacity is the challenging tasks.

Various methods have been proposed for finding the optimal place and capacity for a variety of DG units. Recent advances are mostly based on artificial intelligence and heuristic algorithms. Gozel and Hocaoglu [6] used an analytical technique for the specification of optimum place and capacity of DG to minimize active power losses. This technique is based on equivalent current injection method. Although the computational time of the algorithm is less than that of other techniques, the operational cost of the DG allocation was not considered in the mentioned work. Kollu *et al.* [7] presented a method based on harmony search algorithm (HSA) with a differential operator for the optimal allocation of multiple DG units. This study was conducted only at nominal load without considering light and heavy loads.

Distributed flexible AC transmission system **(**DFACTS) devices are used in the distribution systems with different applications and controlling methods in

Received: 16 Sep. 2015
Revised: 23 De. 2015, 18 Feb., 28 March, and 1 Apr. 2016
Accepted: 16 Apr. 2016
*Corresponding author:
E-mail: hajarbagheri1@gmail.com (H. Bagheri Tolabi)

order to improve the power quality indices. Distributed static compensator (DSTATCOM), unified power flow controller (UPFC), and dynamic voltage restorer (DVR) are more applicable DFACT devices which are widely used in distribution systems. The process of finding optimal location and capacity of the DFACTS devices considerably influences the achievement of higher efficient output from these devices. Tanti *et al.* [8] presented an artificial neural network (ANN) approach for the optimal placement of the DSTATCOM and the DVR in a distribution system. The optimal place of DSTATCOM and DVR was achieved by employing a feed forward neural network trained by post-fault voltage amplitude of three phases at various buses. This method was tested only on a small (14 bus) distribution system and its performance on larger networks was not reported. Jain *et al.* [9] presented a method for the optimal placement of DSTATCOM based on the sensitivity index. In this method, the most unstable bus is chosen as the candidate bus for installing the DSTATCOM. Although the obtained results were compared with or without the DSTATCOM, they were not compared to the results of the other techniques.

Several methods have been proposed for the simultaneous reconfiguration and optimal allocation of the DG or DFACT units in distribution systems [1, 10]. One of the recent works in this area was proposed by Kavousi-Fard and Niknam [11]. In this paper, the authors solved the uncertainty issues associated with the problem of wind turbines reconfiguration using bat algorithm. However, simultaneous reconfiguration of the DG and DFACT units has been rarely reported in the literature. A few studies have investigated the multi-objective optimization problem including reduction in losses, voltage stability improvement, and enhancing load balancing in a distribution system.

In this paper, a novel idea for simultaneous reconfiguration and optimal allocation of both WT and DVR units in a distribution network is proposed (the presence of the wind turbine increases the voltage drop which may lead to voltage instability in the network; a DVR unit along with the wind turbine (WT) is suggested to overcome this problem). Also, a new multi-objective function is proposed for reducing the total power loss and operational cost, while improving the voltage stability and load balancing indices in a distribution system. Furthermore, a hybrid algorithm which combines the simulated annealing (SA) and intelligent water drops (IWD) algorithms is proposed to solve the proposed nonlinear/complex problem. Since the proposed SAIWD method uses a two-stage random selection, the probability of trapping in a local optimum can significantly reduce.

The rest of this paper is organized as follows: The problem is formulated and presented in Section 2. The SA and the IWD approaches are discussed in Section 3. Section 4 explains the optimization procedure using the proposed SAIWD method. Section 5 includes performance evaluation and simulation results. The paper is concluded in Section 6.

2. PROBLEM SPECIFICATION

The problem of simultaneous reconfiguration and placement of the WT and DVR units in a distribution network is formulated in the following sections:

2.1. Load flow mathematical model

An efficient method is used for load flow solution of radial distribution networks [12,13]. The applied load flow method needs only the set of nodes and branch numbers of feeder, all laterals and sub-laterals. The proposed method computes branch load flow more efficiently and does not need to store nodes beyond each branch. The voltage of each node is calculated using a simple algebraic equation (i.e. Equation (2)). Load flow can be computed using the following equations in a distribution system [1, 12-13]:

$$\begin{aligned}
P_{k+1} &= P_k - P_{loss,k,k+1} - P_{Lk+1} \\
&= P_k - \frac{R_{k,k+1}}{|V_k|^2}\left\{P_k^2 + (Q_k + Y_k|V_k|^2)^2\right\} - P_{Lk+1}, \\
Q_{k+1} &= Q_k - Q_{loss,k,k+1} - Q_{Lk+1} \\
&= Q_k - \frac{X_k}{|V_k|^2}\left\{P_k^2 + (Q_k + Y_{k1}|V_k|^2)^2\right\} \\
&\quad - Y_{k1}|V_k|^2 - Y_{k2}|V_{k+1}|^2 - Q_{Lk+1}
\end{aligned} \tag{1}$$

$$\begin{aligned}
|V_{k+1}|^2 &= |V_k|^2 + \frac{R_{k,k+1}^2 + X_{k,k+1}^2}{|V_k|^2}(P_k^2 + Q_k^2) - \\
&\quad 2(R_{k,k+1}P_k + X_{k,k+1}Q_k) \\
&= |V_k|^2 + \frac{R_{k,k+1}^2 + X_{k,k+1}^2}{|V_k|^2}(P_k^2 + (Q_k^2 + Y_k|V_k|^2)^2) - \\
&\quad 2(R_{k,k+1}P_k + X_{k,k+1}(Q_k + Y_k|V_k|^2))
\end{aligned} \tag{2}$$

where,

P_k : Real power of bus *k*,

Q_k : Reactive power of bus *k*,

$P_{loss,k,k+1}$: Loss of real power in line section between buses *k* and *k+1*,

$Q_{loss,k,k+1}$: Loss of reactive power in line section between buses *k* and *k+1*,

P_{Lk+1}: Real power of the load at bus *k+1*,

Q_{Lk+1}: Reactive power of the load at bus *k+1*,

$R_{k,k+1}$: Line section resistance between two consequent buses *k* and *k+1*,

$X_{k,k+1}$: Line section reactance between buses *k* and *k+1*,

Y_k : Shunt admittance of the k-*th* bus and

V_k : Voltage (magnitude and phase) of the k-*th* bus.

2.2. Wind turbine equations

A wind turbine system consists of the following main components: a mechanical drive, a power grid, a controller, and a generator. Wind turbines convert the kinetic energy of wind into mechanical energy. The generator converts the mechanical energy into electrical energy. For a wind turbine unit, the active and reactive powers are computed as follows [13]:

$$P_{WT} = [\frac{V_k^2}{R_k} P_{WT,loss} - (P_k^2 + Q_k^2) - (Q_{WT}^2 - 2P_k P_{WT} - 2Q_k Q_{WT})(\frac{G}{L})]^{1/2} \quad (3)$$

$$Q_{WT} = [\frac{V_k^2}{R_k} P_{WT,loss} - (P_k^2 + Q_k^2) - (P_{WT}^2 - 2P_k P_{WT} - 2Q_k Q_{WT})(\frac{G}{L})]^{1/2} \quad (4)$$

where,
P_{WT} : Real power generated/consumed by the WT
Q_{WT} : Reactive power generated/consumed by the WT
G : Distance between the source and the WT location in *km* and
L: Distance from the source to bus k in *km*

The main components of wind power system are represented in Fig. 1. In this paper, a fixed speed model for wind turbine is considered which is a PQ bus in the load flow analysis.

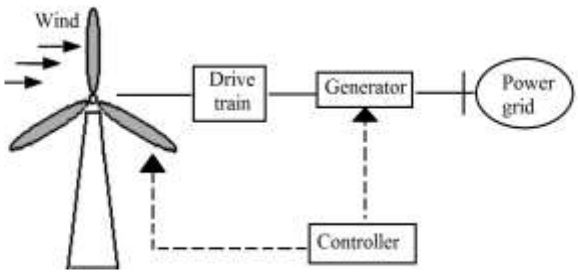

Fig. 1. Main components of the wind power system.

2.3. The DVR equations

The DVR is a DFACT device that consists of a voltage source converter (VSC), harmonic filter, injection transformer, and energy storage and controlling system. The circuit diagram of the DVR is represented in Fig. 2.

Few articles have addressed the issue of how to model DVR for load flow analysis. It is conventionally modeled for load flow calculation as PV or PQ buses, depending on the application. In the load flow analysis, a DVR is treated as a series reactive power controller and can regulate its injected reactive power to control the voltage of its terminal bus. Accordingly in this paper, the DVR is considered a PV bus in the load flow analysis.

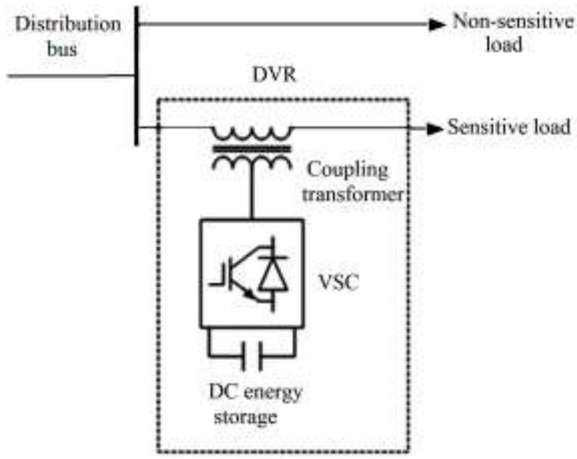

Fig. 2. The DVR circuit diagram.

The series injected voltage of the DVR can be written as [14]:

$$V_{DVR} = V_L + Z_{th} I_L - V_{th} \quad (5)$$

where,
V_L: Magnitude of the load voltage
Z_{th}: Impedance of the load
I_L: Current of the load
V_{th}: System Thevenin voltage

The complex power injection of DVR is computed as:

$$S_{DVR} = P_{DVR} + jQ_{DVR} = V_{DVR} \cdot I_L^* \quad (6)$$

where,
S_{DVR}: Complex power injection of the DVR,
P_{DVR}: Active power injection of the DVR and
Q_{DVR}: Reactive power injection of the DVR

2.4. Multi-objective function

The main objectives are to reduce power loss and improve the voltage stability and load balancing indices. f_1 index reflects the power losses defined as follows:

$$f_1 = \sum_{n_f} \sum_{k=1}^{n_s} R_{k,k+1} \left| I_{k,k+1} \right|^2 \quad (7)$$

where,
ns : Total number of sections for a feeder and
nf : Total number of feeders in a distribution network

The decrease in the f_1 index implies the reduction of power losses in the distribution system.

The second index reflects the voltage stability in the distribution system.

For two nodes of distribution system, the static voltage stability index f_2 can be presented as follows [15]:

$$f_2 = 4[(X_{k,k+1} P_{Lk+1} - R_{k,k+1} Q_{Lk+1})^2 + (X_{k,k+1} Q_{Lk+1} - R_{k,k+1} P_{Lk+1}) V_k^2] / V_k^4 \quad (8)$$

The node which has the minimum f_2 value is the most sensitive one to voltage collapse. Increase in the f_2 index means improvement in the voltage stability of the network.

The third objective of optimization is the line feeders' load balancing index defined as follows [1]:

$$f_3 = \sum_{n_f} \sum_{k=1}^{n_s} \left(\frac{I_k}{\frac{1}{n_s} \sum_{k=1}^{n_s} I_k} \right)^2 \quad (9)$$

where, I_k is the current passing through line k.

The decrease in the f_3 index reflects increasing the load balancing of the network.

The fourth term of objective function aims to minimize the total operational cost (in 24 h). The operational cost is divided into three components [16, 17]. The first component is related to the cost of active power supplied from the substation. This item may be decreased by minimizing the total loss of the system. The second component is related to the cost of active/reactive power supplied by the WT/DVR units. This item can be decreased by minimizing the value of active/reactive power taken from WT/DVR units. The third term is the reconfiguration cost of the system. This item may be minimized by reducing the number of switching operation. Accordingly, the operational cost that can be minimized is as follows:

$$f4 = c_1 \operatorname{cost}_{T,loss} + c_2 \operatorname{cost}_{WT/DVR} + c_3 \operatorname{cost}_{rec} \quad (10)$$

where,

$\operatorname{cost}_{T,loss}$: Cost of active power supplied from the substation in 24 h,

$\operatorname{cost}_{WT/DVR}$: Cost of active/reactive power supplied by the WT/DVR units in 24 h,

$\operatorname{cost}_{rec}$: Cost of switching operation in 24 h and

c_1, c_2 and c_3: Price coefficients of the real/reactive power injected/consumed by substation, the WT/DVR, and reconfiguration in \$/kVA/rec. In this paper, these coefficients are considered 4 \$/kVA, 5 \$/kVA, and 2 \$/rec, respectively [16, 17].

The constraints considered for the multi-objective optimization problem are considered as follows:

$1: V_{k\min} \le V'_k \le V_{k\max}$ (this constraint is related to the voltage which is required to be kept within the standard limit at each bus)

where,

V'_k: Voltage of the k*th* bus for each solution,

$V_{k\max}$: Maximum voltage of the k*th* bus and

$V_{k\min}$: Minimum voltage of the k*th* bus

$2: \left|I'_{k,k+1}\right| \le \left|I_{k,k+1\max}\right|$ (this constraint restricts the current of each branch within the standard limitation)

where,

$I'_{k,k+1}$: Line section current between buses k and $k+1$ after each solution and

$I_{k,k+1\max}$: Maximum line section current between buses k and $k+1$

$3: \sum_{k=1}^{n} P_{(WT+DVR)k} \le \sum_{k=1}^{n} P_{\sigma k}$,

where,

$P_{(WT+DVR)k} = P_{WT_k} + P_{DVR_k}$ and $P_{\sigma k} = P_k + P_{loss,k}$.

where, n is total number of buses. This constraint is related to power injection limitation of the branch. The optimal location and size of the DG and DVR in distribution system is obtained regarding the power balancing constraint.)

4: Radial structure of the network should be maintained.

5: All the available nodes of the considered distribution system should be fed (to satisfy both 4 and 5 constraints simultaneously, a method based on [18] is employed in which a radial distribution network which feeds all of its loads can be considered a tree graph)

According to the above description, the following mathematic relation is defined for the fitness function evaluation of the solution:

$$\begin{aligned} Fitness = \max[(&F_1 + F_2 + F_3 + F_4 + \\ &\alpha_1 \sum_{k\in n} [\max(V'_k - V_k^{\max}, 0) + \\ &\max(V_k^{\max} - V'_k, 0)] + \\ &\alpha_2 \sum_{k\in n} [\max(I'_{k,k+1} - I_{k,k+1\max}, 0) + \\ &\max(I'_{k,k+1} - I_{k,k+1\max}, 0)] + \\ &\alpha_3 \sum_{k\in n} \max(P_{(WT+DVR)k} - P_{\sigma k}, 0) \end{aligned} \quad (11)$$

where,

$F_1 = (f_{1b} - f_1)/f_{1b}$, $F_2 = ((f_2 - f_{2b})/f_{2b})^{-1}$, $F_3 = (f_{3b} - f_3)/f_{3b}$, $F_4 = (f_{4b} - f_4)/f_{4b}$, and $\alpha_1 = \alpha_2 = \alpha_3 = 0.33$ are the penalty coefficients. These coefficients are imposed when constraints are violated. f_{ib} is the base value of the ith objective function. The basic value for all the objectives, except the second objective function (f_{2b}), is considered the maximum amount of each objective. It is clear that the greater amount of F_1, F_2, F_3, F_4 fitness values (i.e. the smaller value of f_1, f_3, f_4 and larger value of f_2) improves the multi-objective function.

3. OPTIMIZATION METHODS

3.1. Simulated annealing (SA) algorithm

The idea of ssimulated annealing was first proposed by Metropolis *et al.* in [19]. In this algorithm, each "*s*" point is assumed as a state of particular system. The function *E(s)* indicates the internal energy of the system in a particular situation. The main objective is to modify the system performance from an initial situation to an optimal situation with the minimum level of energy [20-21].

The change of energy is expressed by ΔE. If $\Delta E \le 0$, the replacement of the atoms is admitted; otherwise, a probability function will determine the chance of the acceptance of the new structure [1, 22]:

$$p(\Delta E) = \exp(\frac{-\Delta E}{k_b.T_k}) \quad (12)$$

where,

k_b : Boltzmann's constant and

T_k : Temperature at time k

The cooling procedure is anticipated to cool down the system faster than the beginning, but slower when the temperature is reduced as specified follows [1, 22]:

$$T_k = \alpha T_0 \quad (13)$$

where

α : Cooling rate

T_0 : Initial temperature

In the probability evaluation procedure, a random number will be chosen within [0, 1]. The selected number will be compared with the $p(\Delta E)$ value. If it is smaller than $p(\Delta E)$, the new structure is accepted; otherwise, it will be rejected. The procedure continues until achieving an equilibrium level.

3.2. Intelligent water drops (IWD) approach

The IWD algorithm tries to mimic the behavior of the swarm of water drops in discovering their ways to the oceans [1, 23].

Each IWD model includes two important parameters:

- Load of soil: $soil^{IWD}$.
- Velocity: Movement velocity of water drops: vel^{IWD}.

These parameters change during the IWD movement. The velocity of water drops is frequently updated on the interval of Δvel^{IWD} from point i to point j as follows [1, 23]:

$$\Delta vel^{IWD} = \frac{a_v}{b_v + c_v[soil(i,j)]^2} \quad (14)$$

where,

$soil(i,j)$: Soil of the edge between points i and j

av, bv, and *cv*: Positive parameters for the IWD algorithm.

The velocity of the drops at $time(t+1)$, is given by [1, 23]:

$$vel_{t+1}^{IWD} = vel_t^{IWD} + \Delta vel^{IWD} \quad (15)$$

where, vel_t^{IWD} is the velocity of the IWD at time t.

The soil load removed from the bed of the edge of $edg(i,j)$ from point i to point j is given as follows [1]:

$$\Delta soil(i,j) = \frac{a_s}{b_s + c_s[time(i,j;vel^{IWD})]^2} \quad (16)$$

where,

as, *bs*, and *cs*: Pre-defined positive parameters for the IWD algorithm and

$time(i,j;vel^{IWD})$ is calculated using Eq. (17):

$$time(i,j;vel^{IWD}) = \frac{HUD(i,j)}{\max(\varepsilon_v; vel^{IWD})} \quad (17)$$

where, $HUD(i,j)$ is a heuristically defined function and ε_v is threshold of velocity [1].

The updated soil and the soil load of the IWD are evaluated using Eqs. (18) and (19), respectively [1, 23].

$$soil(i,j)_{(t+1)} = (1-\rho_n)(soil(i,j)_{(t)} - \rho_n \Delta soil(i,j) \quad (18)$$

where, ρ_n is the local soil updating parameter.

$$soil^{IWD}{}_{(t+1)} = soil^{IWD}{}_{(t)} + \Delta soil(i,j) \quad (19)$$

The edge of an IWD is selected using a probability function as follows [1, 23]:

$$p(i,j;IWD) = \frac{f(soil(i,j))}{\sum_{k \notin v_c(IWD)} f(soil(i,k))} \quad (20)$$

where, $f(soil(i,k)) = 1 + \varepsilon_s + g(soil(i,j))$ and

ε_s is a small positive figure to collate the singularity.

The function $g(soil(i,j))$ is defined as follows:

$$g(soil(i,j)) = \begin{cases} soil(i,j) & if: \min_{l \notin v_c(IWD)} (soil(i,l)) \geq 0 \\ soil(i,j) - \min_{l \notin v_c(IWD)} (soil(i,l)) & otherwise \end{cases} \quad (21)$$

The function $\min(.)$ indicates the minimum values. The best solution of the current best iteration, $T^{IB,}$ is evaluated at the end of each iteration as follows:

$$T^{IB} = \arg\max_{\forall IWDs} q(T^{IWD}) \quad (22)$$

where, T^{IWD}: Solution founded by an IWD, T^{IB} is the current iteration best solution and the function $q(.)$ is the fitness function and T^{IWD} is a solution generated by an IWD.

The $soil(i,j)$ corresponding to T^{IB} is updated using the following equation [1, 23]:

$$soil(i,j) = (1+\rho_{IWD}) soil(i,j) - \rho_{IWD} \frac{1}{N_{IB}-1} soil_{IB}^{IWD}, \quad \forall (i,j) \in T^{IB} \quad (23)$$

where

$soil_{IB}^{IWD}$: The best IWD soil in the current iteration when reaching the destination,

N_{IB}: The number of nodes in the IWD solution and

ρ_{IWD}: Global soil updating parameter [1, 23].

At the end of each iteration, the total best solution T^{TB} is updated based on the T^{IB} as follows:

$$T^{TB} = \begin{cases} T^{TB} & if \quad q(T^{TB}) \geq q(T^{IB}) \\ T^{IB} & otherwise \end{cases} \quad (24)$$

In the IWD algorithm, the above equation guarantees that T^{TB} always contains the best solution discovered so far [1, 23].

4. THE PROPOSED HYBRID SAIWD METHOD

The perceptual diagram of the SAIWD is shown in Fig. 3. First, initial IWD swarms are created according to the IWD structure. Next, using the information provided by the equation of position movement of the

IWD, each IWD moves from the present (*i*) to the next (*j*) positions. Normal IWD automatically accepts this position as the new position of the IWD; however, the SAIWD introduces the SA acceptance rule at this stage. The rule determines whether to accept the new position or recalculate another candidate position, which is conducted according to the fitness function difference between the new and old positions and enables the solution to jump out of local optima and decrease the vibration near the end of a located solution.

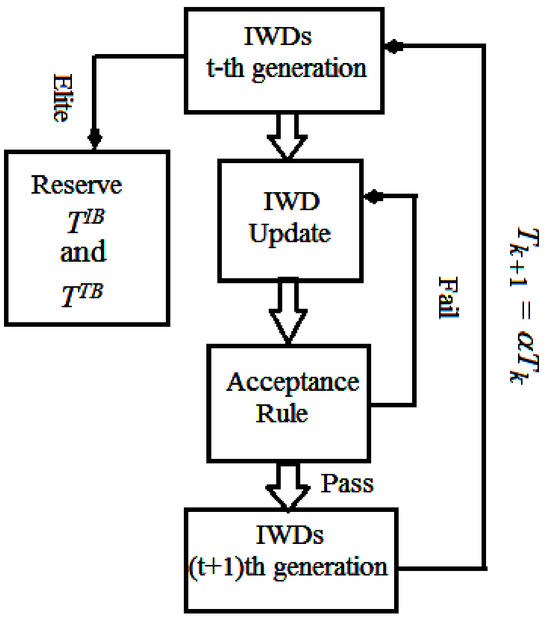

Fig. 3. The SAIWD perceptual diagram.

These characteristics improve the quality of the solution and increase the conversancy rate.

Since the rule for accepting or rejecting a new solution is based on the current temperature parameter and the fitness value difference, the process will explore for the solutions toward the direction of T^{IB} and T^{TB}. If a candidate solution satisfies the related criteria, then a new position is computed using the IWD (similar to the disturbance mechanism in the SA); this procedure is repeated until the rule accepts the new position or the upper limit of disturbances is achieved. In this way, the algorithm can explore more solutions on the paths by increasing the probability that leads to achieving the global optima. In addition, the parallel processing capabilities of the IWD reduce calculation time. Since the proposed hybrid method uses random selection twice, therefore, the probability of trapping in a local optimum is significantly reduced.

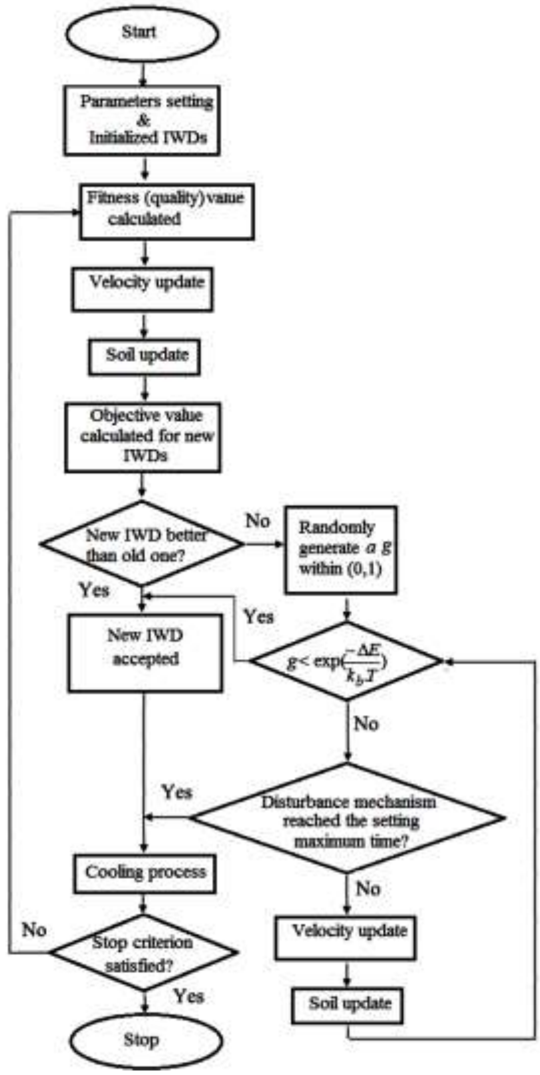

Fig. 4. The flowchart of proposed SAIWD algorithm.

The details of the flowchart of the SAIWD algorithm are presented in Fig. 4 and the whole procedure of the SAIWD is described as follows:

Step 1: Set all the parameters, including as, bs, cs, a_v, b_v, c_v; Initsoil, Initvel, N_{IB}, ρ_{IWD}, ρ_n, MaxIter, initial temperature T_0, cooling rate (α), and set $\text{Itercount} = t = 0$. Initialize IWDs randomly.

Step 2: Calculate soil $soil^{IWD}{}_t$ and velocities vel_t^{IWD} for each IWD_i.

Step 3: Calculate the fitness value ($q(T^{IWD})$) of all IWDs and determine the values of T^{IB} and T^{TB} for the t-th solution.

Step 4: Evaluate $\Delta q_i = q(T^{IWD_i})_{t+1} - q(T^{IWD_i})_t$ and select a random number $g \in [0,1]$. If $\Delta q_i < 0$, it means that the new solution is improved for optimizing fitness function; then, it is accepted as the new status of IWD_i. Otherwise, T^{IWD_i} is accepted if $g < \exp(\frac{\Delta q_i}{T_k})$.

Step 5: If the soil load and velocity of all the IWDs are determined, go to Step 6; else, return to Step 2 for those IWDs that have no chance for being accepted and generate new soils and velocities using the similar procedure.

Step 6: Update each IWD status to the new status and modify T^{IB} and T^{TB} by comparing their fitness values.

When the evolution process reaches the stopping criteria, go to Step 7; otherwise, let $t = t + 1$ and $T_{k+1} = \alpha T_k$ and then go to Step 2.

Step 7: Print the best solution T^{TB}.

5. SIMULATION AND NUMERICAL RESULTS

For the performance evaluation of the hybrid SAIWD algorithm, the proposed approach is implemented in MATLAB. The testing system employs the Taiwan Power Company (Tai-Power Company) 11.4-kV distribution system at the nominal load level.

For the nominal load level, six different scenarios are considered to analyze the effectiveness of the proposed hybrid approach as follows:

Scenario I: Test the system without the reconfiguration and allocation of the WT and the DVR units.

Scenario II: Test the system only with reconfiguration.

Scenario III: Test the system with optimal WT allocation.

Scenario IV: Test the system with optimal DVR allocation.

Scenario V: Test the system with simultaneous WT and DVR allocation and without reconfiguration.

Scenario VI: Test the system with simultaneous reconfiguration and allocation of the WT and DVR.

For the scenarios including the WT or DVR, the maximum capacity of 3 MVA is considered for the WT or DVR installation.

The choice of parameters is determined using a trial and error process. The selected parameters for the simulation are as follows:

as, *cs*, *av*, and *cv*=1, *b* and *bs*=0.01, *Initsoil*=3000, Initvel=100, *MaxIter*=100, ρ_{IWD}=0.85, ρ_n=0.89, ε_s=0.001, $q(T^{IWD}) = -\infty$, Temperature steps=50, α=0.98, and T_0=300k.

5.1. Evaluation process

For the evaluation purpose, a testing procedure is conducted. The test system is a real distribution network from Taiwan Power Company (TPC), the details of which are provided in [24]. This practical 11.4-kV system was equipped with 83 sectionalizing switches and 13 tie switches. The total system load, which was considered balanced and constant, was 28.35 MW and 20.7 MVAr, respectively. More details could be found in [24]. The load flow was calculated based on S_{base}=100 MVA and V_{base}= 11.4 kV.

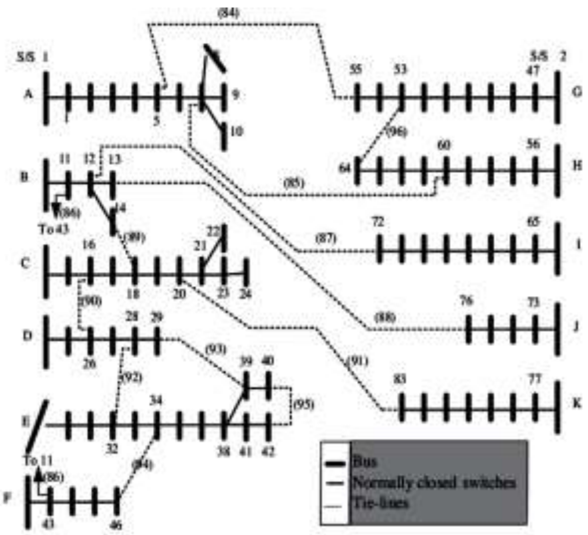

Fig. 5. Taiwan Power Company test system.

5.2. Obtained results

The results of the proposed approach for scenarios II to VI are presented in Table 1.

It is observed in Table 1 that base power loss (f_1 index) is 531 kW which is reduced to 371.34, 338.06, 365.27, 302.58, and 281.72 kW using scenarios II to VI, respectively.

f_2 (i.e. voltage stability index) is calculated as 0.92, 0.95, 0.91, 0.96, 0.97, and 0.99 and f_3 (load balancing index) is obtained as 140.4, 109.73, 97.05, 104.62, 95.21, and 91.16 for scenarios I to VI, respectively. f_4 (operational cost function) is computed as 7663, 7155, 6935, 7089, and 5847 \$ for scenarios II to VI, respectively. Also, Table 1 includes the optimal location and size for WT and DVR units for scenarios III to VI. The obtained results for f_1, f_2, and f_3 indices are compared to the base system (scenario I) and the results are presented in Fig. 6 for scenarios II to VI. Furthermore, in this figure, the obtained results are compared using the calculated f_4 values for scenarios II to VI.

By comparing the obtained results from Table 1 and Fig. 6, the following conclusions are made:

- It is confirmed that, by applying the proposed SAIWD approach, the active power loss is reduced and load balancing indexes are improved for all the indices in scenarios II to VI.
- It can be seen in Table 1 and Fig. 6 that maximum improvement in all the four f_1, f_2, f_3, and f_4 indices is achieved based on scenario VI. This result proves the superiority of scenario VI, i.e. proposed hybrid approach, to other scenarios.
- According to Fig. 6 (a), (b), (c), and (d), the best results are obtained based on scenario VI (simultaneous reconfiguration with WT and DVR allocation) and scenario V (simultaneous WT and DVR allocation), respectively. Comparing various results obtained from different scenarios involving reconfiguration, the WT or DVR allocation, and hybrid model, it is revealed that

simultaneous reconfiguration with WT and DVR allocation, or simultaneous WT and DVR allocation are more superior to their single-objective optimization model.

- Voltage stability index is improved for scenarios II, IV, V, and VI, while it is deteriorated in scenario III. It means that, although the allocation of the WT units within the distribution system improves the loss reduction and load balancing indices, it may reduce the voltage stability of the network. This result seems to be reasonable, because the WT unit can inject the active power; on the other hand, it may feed from the reactive power of the network. The system voltage stability index is decreased due to the reactive power decrease [25]. If the WT consumes a large quantity of the reactive power, it can lead to voltage instability.

Table 1. SAIWD results for the TPC test system

Scenario	Tie (open) switches	WT size (MVA) @ bus	DVR size (MVA) @ bus	f_1*(kw)*, f_2*(p.u)*, f_3 and f_4*($)* values
II	7, 13, 34, 39, 55, 62, 72, 83, 86, 89, 90, 92, 95	-	-	387.2, 0.93, 112.61, 7663
III	84, 85, 86, 87, 88, 89, 90, 91, 92, 93, 94, 95, 96	2.617 @ 79	-	354.85, 0.90, 106.42, 7155
IV	84, 85, 86, 87, 88, 89, 90, 91, 92, 93, 94, 95, 96	-	1.837@ 8	382.31, 0.94, 110.76, 6935
V	7, 13, 34, 39, 41, 61, 84, 86, 87, 89, 90, 91, 92	1.865 @ 20	1.523@ 9	341.764, 0.95, 102.68, 7089
VI	7, 13, 34, 39, 42, 55, 72, 86, 89, 90, 91, 92, 96	2.457 @ 20	1.749@ 10	319.28, 0.97, 97.58, 5847

- As shown in Table 1 and Fig. 6, although both scenarios III and V contain a WT unit, the results of scenario V are better than those of scenario III (especially, in improving the voltage stability index). As in scenario V, a DVR unit is allocated along with the wind turbine. It can be concluded that the use of a DVR unit can solve the voltage instability problem produced by wind turbine.
- From Fig. 6 (a) and Fig. 6 (c), it is observed that the loss reduction and load balancing improvement based on scenario III are greater than the corresponding values based on scenarios II and IV. It means that, in order to reduce power losses or increase load balancing, the use of WT units can be more effective than the reconfiguration or placement of DVR unit.
- From Fig. 6 (b), it is observed that the voltage stability based on scenario IV is greater than the corresponding values based on scenarios II and III. It means that, in order to only improve voltage stability, the DVR units can be more efficient than reconfiguration or the WT unit allocation.
- Among all the scenarios, the maximum and minimum operational cost values are obtained for scenarios II and VI, respectively.

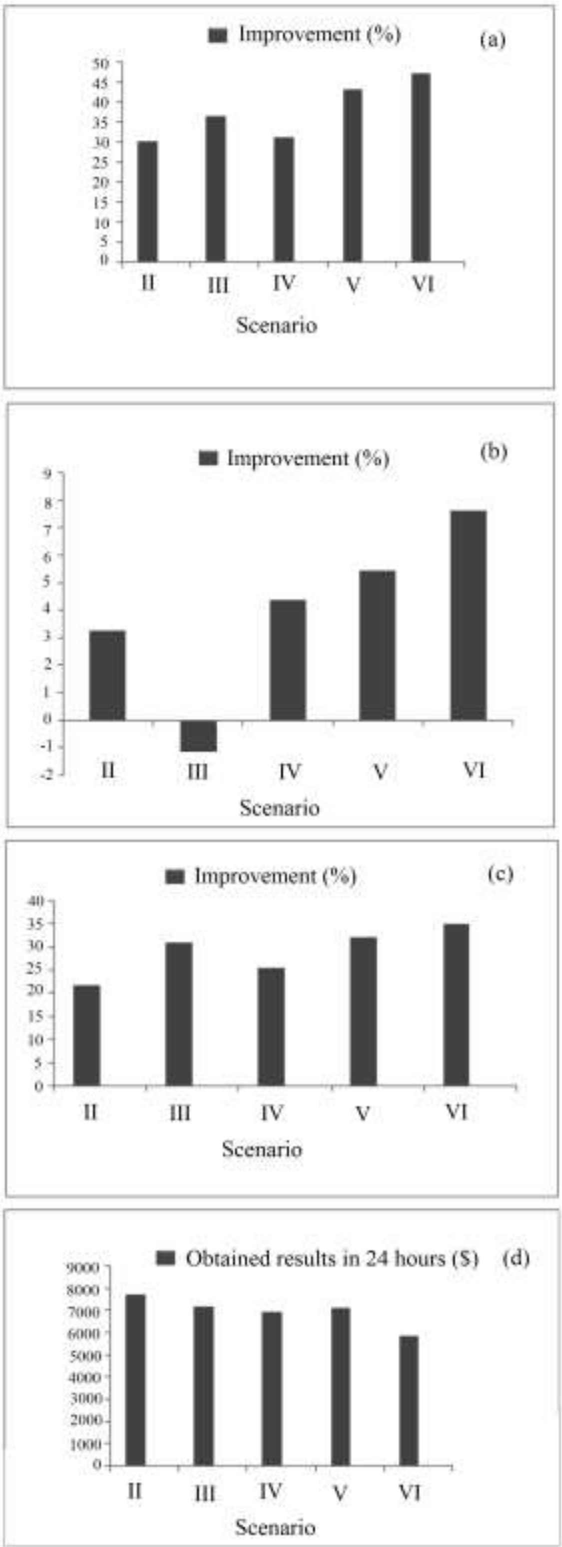

Fig. 6. Comparison of the obtained results for (a) f_1, (b) f_2, (c) f_3 and f_4 indices improvement.

It means that: 1) Among single-objective optimization models (i.e. scenarios II to IV), although it seems the initial cost of the reconfiguration is less than the WT or DVR installation, the implementation of scenario II can save less for the future costs of distribution system than the WT or DVR installation (the reason could be less power loss reduction and inability to inject the power into the grid of this scenario); and 2) Although it seems the initial cost of scenario VI is more than that of others, the implementation of scenario VI can lead to the most economical saving in the future costs of distribution system, compared with other scenarios (because by adding WT and DVR units along with reconfiguration, on the one hand, the power loss and its cost will significantly reduce and, on the other hand, the purchased power from transmission lines is reduced, which leads to the minimization of the total operational costs).

Results of the IWD approach without optimization by the SA algorithm on the TPC test system are shown in Table 2.

As can be observed, the power loss index (f_1) is estimated as 387.2, 354.85, 382.31, 341.764, and 319.28 kW, voltage stability index (f_2) is calculated as 0.93, 0.90, 0.94, 0.95, and 0.97, and load balancing index (f_3) is obtained as 112.61, 106.42, 110.76, 102.68, and 97.58 for scenarios II to VI, respectively. f_4 (operational cost function) values are 8405, 7764, 7325, 8119, and 6291 $ for scenarios II to VI, respectively. These results prove that the performance of SAIWD approach is better than that of the IWD.

The obtained results on the TPC test system show that bus No. 9 is more sensitive than other buses. In the base case, the voltage magnitude of this bus is 0.928 p.u. However, this bus is the weakest bus of the system and it is more subjected to voltage collapse in the case of load variation.

Table 2. IWD results for the TPC test system

Scenario	Tie (open) switches	WT size (MVA) @ bus	DVR size (MVA) @ bus	f_1(kw), f_2(p.u), f_3 and f_4($) values
I	84, 85, 86, 87, 88, 89, 90, 91, 92, 93, 94, 95, 96	-	-	531, 0.92, 140.4, -
II	7, 13, 34, 39, 41, 61, 84, 86, 87, 89, 90, 91, 92	-	-	371.34, 0.95, 109.73, 8405
III	84, 85, 86, 87, 88, 89, 90, 91, 92, 93, 94, 95, 96	2.941 @ 20	-	338.06, 0.91, 97.05, 7764
IV	84, 85, 86, 87, 88, 89, 90, 91, 92, 93, 94, 95, 96	-	1.903 @ 9	365.27, 0.96, 104.62, 7325
V	7, 13, 34, 39, 41, 61, 84, 86, 87, 89, 90, 91, 92	2.735 @ 22	1.876 @ 9	302.58, 0.97, 95.21, 8119
VI	7, 13, 34, 39, 42, 55, 72, 86, 89, 90, 91, 92, 96	2.676 @ 20	1.854 @ 10	281.72, 0.99, 91.16, 6291

After bus No. 9, buses No. 10 and 8 are more subjected to voltage collapse. The voltage magnitude of these two buses, i.e. bus No. 10 and bus No. 8, is 0.929 and 0.930 pu, respectively. The voltage magnitude curves for buses No. 8, 9, and 10 are shown in Fig. 7(a) for scenario I (i.e. the base system without any optimization) when a fault is accrued at the weakest buses at t=1 sec and is cleared at t=5 sec.

As seen in this figure, the voltage of buses No. 8, 9, and 10 from the beginning to end experiences some oscillations that lead to voltage instability.

Also, it can be seen in Fig. 7(b) that, by the simultaneous reconfiguration with optimal allocation of the WT and DVR units, i.e. scenario VI, the voltage magnitude of the three weak buses is increased and the oscillations are entirely damped.

For the performance evaluation of the proposed method at different load levels, the TPC test system is simulated at three load levels, i.e. 0.5 (light), 1.0 (nominal), and 1.6 (heavy) for scenarios I and VI.

The obtained results are presented in Table 3. It can be seen in Table 3 that, at the light load, the base case f_1 index is 123.77 which is reduced to 104.16 for scenario VI. At the light load, the base case f_2 index is 0.96 which is ameliorated to 1.00 and the f_3 index for the base case is 108, which is improved to 84.25 for scenario VI. Also, at this load level, f_4 is computed as 3937 $ for scenario VI. Similarly, it can be seen in Table 3 for heavy load that, three f_1, f_2, and f_3 indices are improved for scenario VI in comparison with the base scenario.

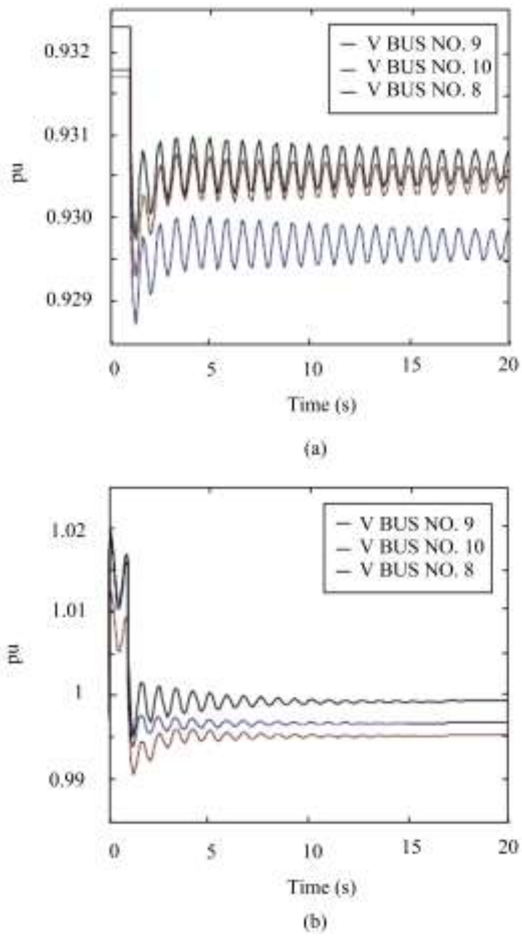

Fig. 7. Comparison of voltage magnitude of buses No. 8, 9 and 10 (a) under the fault condition: for the base system (i.e. scenario I) and (b) after applying the proposed method (i.e. scenario VI).

Table 3. The obtained results for different lad levels on the TPC test system

Item		Load level		
		Light (0.5)	Nominal (1)	Heavy (1.6)
Scenario I	Tie (open) switches	7, 13, 34, 39, 41, 61, 84, 86, 87, 89, 90, 91, 92	84, 85, 86, 87, 88, 89, 90, 91, 92, 93, 94, 95, 96	84, 85, 86, 87, 88, 89, 90, 91, 92, 93, 94, 95, 96
	$f_1(kw)$	123.77	531	1508.73
	$f_2(p.u)$	0.96	0.92	0.83
	f_3	108	140.4	185.02
	$f_4(\$)$	-	-	-
Scenario VI	Tie (open) switches	7, 13, 34, 39, 42, 55, 72, 86, 89, 90, 91, 92, 96	7, 13, 34, 39, 42, 55, 72, 86, 89, 90, 91, 92, 96	7, 13, 34, 39, 41, 61, 84, 86, 87, 89, 90, 91, 92
	$f_1(kw)$	104.16	281.72	1273.43
	$f_2(p.u)$	1.00	0.99	0.91
	f_3	84.25	91.16	154.87
	$f_4(\$)$	3937	5847	11269

Also, the value of f_4 index, at the heavy load level, is shown in Table 3 for scenario VI. The obtained results reveal the superiority of the proposed approach in the case of various load levels. Scenario VI is also simulated at nominal load using genetic algorithm (GA) [4] and particle swarm optimization (PSO) [26].

Table 4. Comparison of simulation results for different approaches.

Method	GA [4]	Tie (open) switches	7, 13, 34, 39, 42, 55, 72, 86, 89, 90, 91, 92, 96
		$f_1(kw)$	301.32
		$f_2(p.u)$	0.93
		f_3	112.45
		$f_4(\$)$	6156
		WT size(MVA) @ bus	2.380 @ 21
		DVR(MVA) @ bus	1.706 @ 10
	PSO [26]	Tie (open) switches	7, 13, 34, 39, 41, 61, 84, 86, 87, 89, 90, 91, 92
		f_1	298.56
		f_2	0.95
		f_3	108.23
		$f_4(\$)$	5934
		WT size(MVA) @ bus	2.416 @ 21
		DVR(MVA) @ bus	1.793 @ 8
	SAIWD (proposed method)	Tie (open) switches	7, 13, 34, 39, 42, 55, 72, 86, 89, 90, 91, 92, 96
		$f_1(kw)$	281.72
		$f_2(p.u)$	0.99
		f_3	91.16
		$f_4(\$)$	5847
		WT size(MVA) @ bus	2.676 @ 20
		DVR(MVA) @ bus	1.854 @ 10

The results are compared with the results obtained using the proposed SAIWD algorithm. It is observed that the SAIWD approach outperforms other counterpart algorithms such as GA and PSO algorithms.

The results of different methods based on scenario V are presented in Table 4.

As shown in Table 4, the value of f_1 index is calculated as 301.32, 298.56 and 281.72 kW, the value of f_2 index is obtained as 0.93, 0.95, and 0.99 p.u, the value of f_3 index is obtained as 112.45, 108.23, and 91.16, the value of f_4 is 6156, 5934, and 5847 \$ using GA, PSO, and SAIWD approaches, respectively. From Table 4, it can be concluded that the SAIWD method is superior to the GA and the PSO algorithms in all terms of loss reduction, operational cost minimization, and improving voltage stability and load balancing.

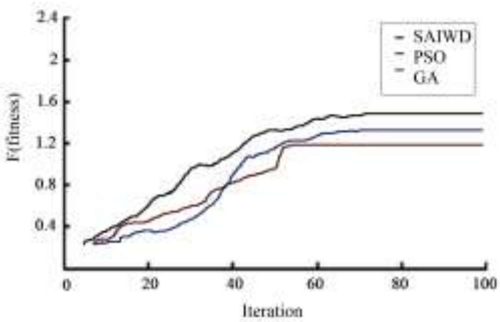

Fig. 8. The convergence behavior of fitness function (*F*) improvements by GA [4], PSO [26] and proposed SAIWD approaches for scenario VI.

Fig. 8 shows the convergence behavior of fitness function (F) using the GA, PSO, and SAIWD methods for scenario VI. Therefore, the SAIWD approach with the final fitness value F=1.48, has a better convergence behavior than the PSO and the GA with the final fitness values of 1.31 and 1.19, respectively.

6. CONCLUSION

In this paper, the SAIWD algorithm is presented for simultaneous reconfiguration and allocation of the WT and DVR units in the distribution system. The proposed approach is employed to reduce the power loss, minimize operating cost, improve voltage stability, and ameliorate load balancing of the feeder. To evaluate the effectiveness of the proposed approach, six different scenarios are tested on a real distribution network, i.e. Taiwan Power Company. At the nominal load, the loss reduction is 46.9% and also voltage stability and load balancing improvements are 7.6% and 35.07%, respectively, compared with the base system. Also, by comparing the results of the operational cost of various scenarios, it is observed that the simultaneous reconfiguration and allocation of the WT and the DVR units based on the SAIWD method, with the total cost of 5847 \$, will lead to the most economical saving in the future costs of the distribution system. By comparing the results, it is found that the installation of the WT unit is more efficient than the reconfiguration or DVR unit allocation for loss reduction or load balancing improvement, while the implementation of the DVR unit is more efficient than reconfiguration or the WT allocation for the voltage stability improvement. The evaluation of different scenarios shows the allocation of the WT unit may reduce the voltage stability of the network and this problem can be solved by the use of the DVR along with wind turbine unit. From the obtained results, it is revealed that the proposed SAIWD approach outperforms the IWD, GA, and PSO approaches in all the terms of the loss reduction, while minimizing the operating cost and improving the voltage stability and load balancing indices in the distribution system.

FUTURE WORKS

In this study, uncertainty sources associated with the wind turbine power generation were ignored. The future works could extend the proposed method by managing the uncertainties in the output of the wind turbine power.

REFERENCES

[1] H. B. Tolabi, R. Hosseini, M. R. Shakarami "A robust hybrid fuzzy-simulated annealing-intelligent water drops approach for tuning a distribution static compensator nonlinear controller in a distribution system," *Eng. Optim.*, vol. 48, no. 6, pp. 999-1018, 2016.

[2] M. Sedighizadeh, M. Mahmoodi "Optimal reconfiguration and capacitor allocation in radial distribution systems using the hybrid shuffled frog leaping algorithm in the fuzzy framework," *J. Oper. Autom. Power Eng.*, vol. 3, no. 1, pp. 56-70, 2015.

[3] A. Merlin, H. Back "Search for a minimal-loss operating spanning tree configuration in an urban power distribution system," in Proce. of the *PSCC*, Cambridge, 1975, pp.1-18.

[4] K. Nara, A. Shiose, M. Kitagawa, T. Ishihara "Implementation of genetic algorithm for distribution system loss minimum reconfiguration," *IEEE Trans. Power Delivery*, vol. 7, no.3, pp.1044-1051, 1992.

[5] B. Venkatesh, R. Ranjan "Optimal radial distribution system reconfiguration using fuzzy adaptation of evolutionary programming," *Int. J. Electr. Power Energy Syst.*, vol. 25, no. 10, pp. 775-780, 2003.

[6] T. Gözel T, M. Hakan Hocaoglu "An analytical method for the sizing and siting of distributed generators in radial systems," *Electr. Power Syst. Res.*, vol. 79, no. 6, pp. 912-918, 2009.

[7] R. Kollu, S. R. Rayapudi, V. L. N. Sadhu "A novel method for optimal placement of distributed generation in distribution systems using HSDO," *Int. Trans. Electric. Energy Syst.*, vol. 24, pp. 547-561, 2014.

[8] D. K. Tanti, M. K. Verma, B. Singh, O. N. Mehrotra, "An ANN based approach for optimal placement of DSTATCOM and DVR in power system for voltage sag mitigation under faults," presented at the *AIATA*, IT-BHU Varanasi, 2011.

[9] A. Jain, A. R. Gupta, A. Kumar "An efficient method for D-STATCOM placement in radial distribution system," in Proce of the *IICPE*, pp. 1-6, 2014.

[10] H. B. Tolabi, M. H. Ali, M. Rizwan "Novel hybrid fuzzy-intelligent water drops approach for optimal feeder multi objective reconfiguration by considering multiple-distributed generation," *J. Oper. Autom. Power Eng.*, vol. 2, no. 2, pp. 91-102, 2014.

[11] A. Kavousi-Fard, T. Niknam "Multi-objective stochastic distribution feeder reconfiguration from the reliability point of view," *Energy*, vol. 64, pp. 342-354, 2014.

[12] H. B. Tolabi, M. H. Ali, S. B. M. Ayob, M. Rizwan "Novel hybrid fuzzy-Bees algorithm for optimal feeder multi-objective reconfiguration by considering multiple-distributed generation," *Energy*, vol. 71, pp. 507-515, 2014.

[13] R. Srinivasa Rao, K. Ravindra, K. Satish, S. V. L. Narasimham "Power loss minimization in distribution system using network reconfiguration in the presence of distributed generation," *IEEE Trans. Power Syst.*, vol. 28, no. 1, pp. 317-325, 2013.

[14] K. Bhumkittipich, N. Mithulananthan "Performance enhancement of DVR for mitigating voltage sag/swell using vector control strategy," *Energy Procedia*, vol. 9, pp. 366-379, 2011.

[15] H. Chen, J. Chen, D. Shi, X. Duan "Power flow study and voltage stability analysis for distribution systems with distributed generation," in Proc. of the *IEEE PES General Meeting*, pp. 1-8, 2006.

[16] K.R. Devabalaji, K Ravi "Optimal size and siting of multiple DG and DSTATCOM in radial distribution system using bacterial foraging optimization algorithm," *Ain Shams Eng. J.*, vol. 7, no. 3, pp. 959-971, 2016.

[17] S. Chandramohan, N. Atturulu, R.P. Kumudini Devi, B. Venkatesh "Operating cost minimization of a radial distribution system in a deregulated electricity market through reconfiguration using NSGA method," *Int. J. Electr. Power Energy Syst.*, vol. 32, no. 2, pp. 126-132, 2010.

[18] Power System Analysis, 1rd ed., McGraw-Hill Co., New York, US, 1994.

[19] N. Metropolis, A. W. Rosenbluth, M. N. Rosenbluth, A. H. Teller, E. Teller "Equation of state calculations by fast computing machines," *J. Chem. Phys*, vol. 21, no. 6, pp. 1087-1092, 1953.

[20] S. Kirkpatrick, C. D. Gelatt, M. P. Vecchi "optimization by simulated annealing," *Science*, vol. 220, no. 4598. pp. 671-680, 1983.

[21] V. Cerny "A thermodynamical approach to the travelling salesman problem: an efficient simulation algorithm," *J. Optimiz. Theory App.*, vol. 45, pp. 41-51, 1985.

[22] M. Gandomkar, H. B. Tolabi "Investigation of simulated annealing, ant-colony and genetic algorithms for distribution network expansion planning with distributed generation," in Proce of the *WSEAS*, pp. 48-52, 2010.

[23] S. H. Hosseini "The intelligent water drops algorithm: a nature-inspired swarm-based optimization algorithm," *Int. J. Bio-Inspir Comput.*, vol. 1, no. 1/2, pp. 71-79, 2009.

[24] L.W. Oliveira, S. Carneiro, E.J. Oliveira, J.L.R. Pereira, I.C. Silva, J.S. Costa, "Optimal reconfiguration and capacitor allocation in radial distribution systems for energy losses minimization," *Int. J. Electr. Power Energy Syst.*, vol. 32, pp. 840-848, 2010.

[25] New Methods To Protect Wind Generators During Voltage Dips Developed, Basque Research, 2015.

[26] J. Olamaei, T. Niknam, G. Gharehpetian, "Application of particle swarm optimization for distribution feeder reconfiguration considering distributed generators," *Appl. Math. Comput.*, vol. 201, no.1-2, pp. 575-586, 2008.